

Thesis Report

Abstract:

Megathrust earthquake sequences significantly impact buildings and infrastructure through the mainshock and trigger aftershocks along the subduction interface and the overriding crust. Although numerous seismic hazard studies have been conducted, essential parameters influencing these events remain insufficiently explored. This study applied the Epidemic-Type Aftershock Sequence (ETAS) model to identify critical seismicity parameters in the Andaman-Sumatra region, focusing on earthquakes above 4 magnitudes from 1960 to 2024. Our analysis demonstrates key relationships between ETAS parameters—including Temporal Decay (γ), Time Decay (c), Spatial Distance (d), Background Seismicity (μ), Omori Law Decay (τ), Spatial Decay (ω), and Productivity (α)—and geological features of the Andaman-Sumatra trench, such as Subduction plate age, trench sediment thickness, short-wavelength Seafloor roughness, convergence velocity, divergence velocity, and subduction velocity of plate. An attempt was also made to find a correlation between relative plate velocity and seismicity rate, revealing a positive relationship: as relative plate velocity increases, the seismicity rate follows suit (Satoshi Ide NGEO1901). Our study identified a key finding: as the subducting plate ages, the spatial distance of aftershocks increases. This suggests that As oceanic plates ages, they become cooler, denser, and more rigid, allowing them to accumulate more stress before fracturing. This results in larger seismic events, with stress spreading over wider areas, leading to a broader spatial distribution of aftershocks. Moreover, we found that temporal decay decreases with plate age, indicating that aftershocks persist for longer durations but occur less frequently as time progresses after the mainshock. These findings provide valuable insights into the complex dynamics of megathrust earthquake sequences in the Andaman-Sumatra region and contribute to a better understanding of the factors controlling seismic hazards in subduction zones.

1. Introduction

The Andaman Sea Trench is located along the convergent boundary between the Indo-Australian and Eurasian plates in the northeastern Indian Ocean. This region experiences intense tectonic activity due to the subduction of the Indo-Australian plate beneath the Eurasian plate, leading to frequent and often large-magnitude earthquakes. These seismic events pose significant risks to the densely populated coastal regions surrounding the trench, including parts of Southeast Asia. Given the high seismic hazard in this region, understanding the underlying mechanisms that drive seismicity is crucial for practical earthquake hazard assessment and mitigation.

One of the primary tools used in seismic hazard analysis is the Epidemic-Type Aftershock Sequence (ETAS) model, which provides a robust statistical framework to examine the temporal and spatial distribution of earthquakes, especially the complex dynamics of aftershocks following significant seismic events. By simulating the clustering behaviour of earthquakes, ETAS helps predict aftershock sequences and offers valuable insights into how these events propagate over time and space. This capability is vital for risk assessment, as aftershocks can often cause additional damage to already weakened infrastructure. In this study, we utilised the ETAS model to identify critical seismic parameters that govern the behaviour of aftershock sequences in the Andaman Sea Trench, enhancing our understanding of the region's seismicity.

However, catalog incompleteness is one of the major problems in seismological studies. The origin of this incompleteness is generally attributed to the limited sensitivity and coverage of the Earth by station networks [Kagan, 2003]. The completeness problem is generally addressed by considering a magnitude threshold (M) above which the frequency-magnitude distribution follows the Gutenberg-Richter relationship [Woessner et al., 2005; Gutenberg et al., 1944]. The number of earthquakes of magnitude m scales as $10^{-b_{val}m}$ (Gutenberg-Richter law), and the number of earthquakes triggered by a typical earthquake of magnitude m scales as $10^{\alpha m}$ (fertility law, as formulated in ETAS model), where $\alpha = \frac{a}{\log 10}$. Where a is the magnitude scaling parameter. Therefore, the total number of earthquakes triggered by all earthquakes of magnitude m scales as, $10^{(\alpha - b_{val})m}$ where $b = \frac{\beta}{\ln 10}$, β is the exponent in the GR law with basis e.

To carry out this analysis, we compiled a comprehensive seismic dataset covering the Andaman Sea Trench from 1960 to 2024, focusing on earthquakes with magnitudes above 4. The ETAS model allowed us to estimate essential seismic parameters, including Temporal Decay (γ), Time Decay (c), Spatial Distance (d), Background Seismicity (μ), Omori Law Decay (τ), Spatial Decay (ω), and Productivity (α). These parameters provide critical insights into earthquake clustering behaviour, shedding light on how tectonic stress is released through a series of aftershocks following major earthquakes. Understanding these patterns is key to improving earthquake hazard models and developing strategies to minimise the risks posed by seismic activity in the region.

Moreover, we investigated the relationship between these ETAS parameters and the Andaman-Sumatra Trench's various geological and tectonic features to deepen our analysis. The transect parameters we explored can be grouped into three major categories: structural, slab, and kinematic.

- **Structural parameters** include trench sediment thickness and short-wavelength seafloor roughness, which offer insights into the physical characteristics of the subduction zone. These features are crucial for understanding how seismic energy propagates and how tectonic stress is distributed across the subduction interface.

- **Slab parameters** primarily focus on the age of the subducting plate, which plays a significant role in determining the slab's thermal and mechanical properties. Older plates tend to be cooler, denser, and more rigid, affecting how stress accumulates and releases during seismic events. This can influence both the magnitude and frequency of earthquakes and aftershocks.
- **Kinematic parameters** encompass subduction velocity, convergence velocity, and deformation rates between the tectonic plates. These parameters provide a dynamic view of the forces driving the subduction process, shedding light on how rapidly the plates move and deform, influencing the region's seismic activity.

By correlating ETAS parameters with these transect parameters, we aim to uncover the physical conditions contributing to the Andaman-Sumatra region's seismicity. This approach offers a more comprehensive understanding of how tectonic and geological factors interact to influence earthquake behaviour, ultimately improving the predictive capability of the ETAS model. The insights gained from this study are crucial for refining seismic hazard assessments and formulating more effective risk mitigation strategies in this highly active seismic zone.

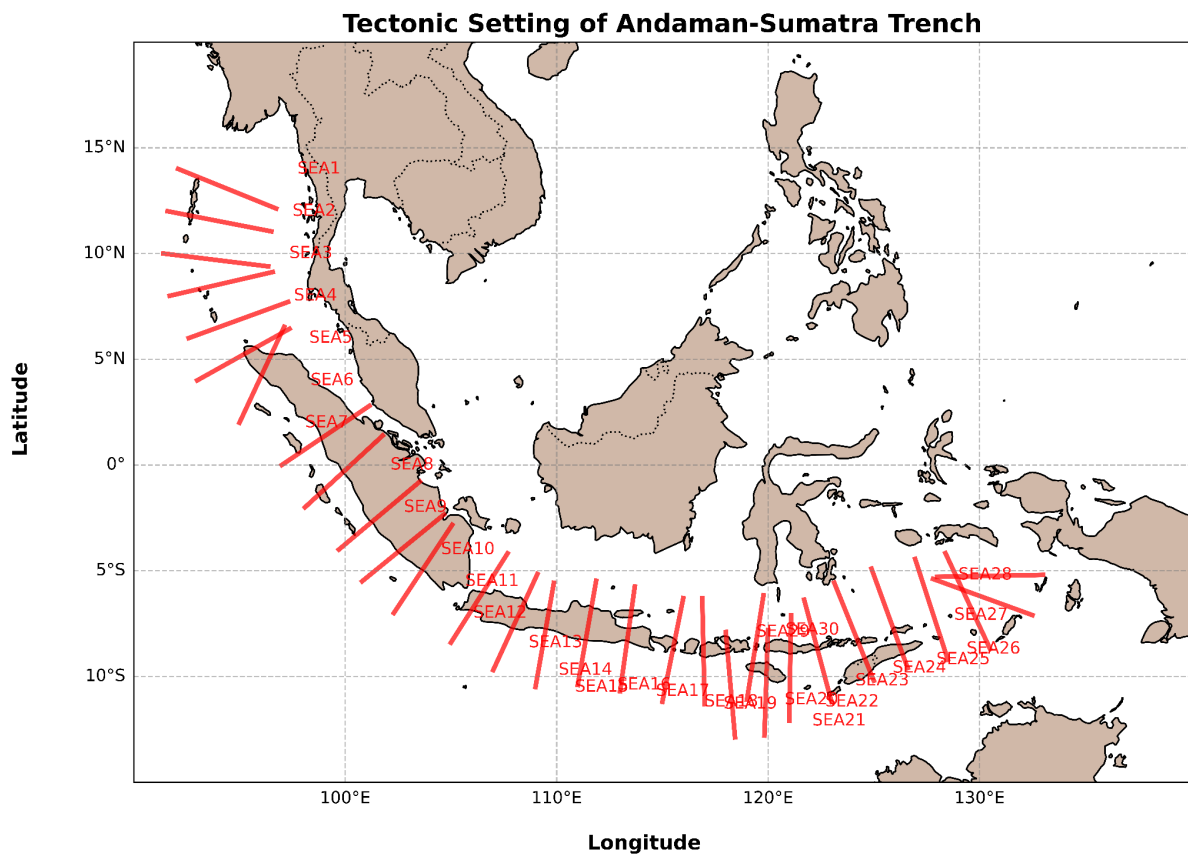


Fig.1: This figure depicts the Andaman-Sumatra Trench, an important subduction zone in the Indian Ocean. It includes several transects that provide detailed cross-sections of the trench, highlighting its geographical extent and boundaries. The displayed transects help to visualise the trench's structure and its relation to other tectonic features in the region.

2. Data

The seismic data used in this study are obtained from the **Incorporated Research Institutions for Seismology (IRIS)** (<https://www.iris.edu/hq/>). We selected the time window between 1960 and 2024 as the investigation period, with the previous 10 windows, 1960 to 1970, as the auxiliary window. This study includes events between 22.09 S to 17.73 N latitudes and 81.84 E to 142.92 E longitudes, encompassing the Andaman Sea transects. The moment magnitude of the events observed ranges between 0 to 9. A total of 84803 events of magnitude between above 4 to 9 were included in our study.

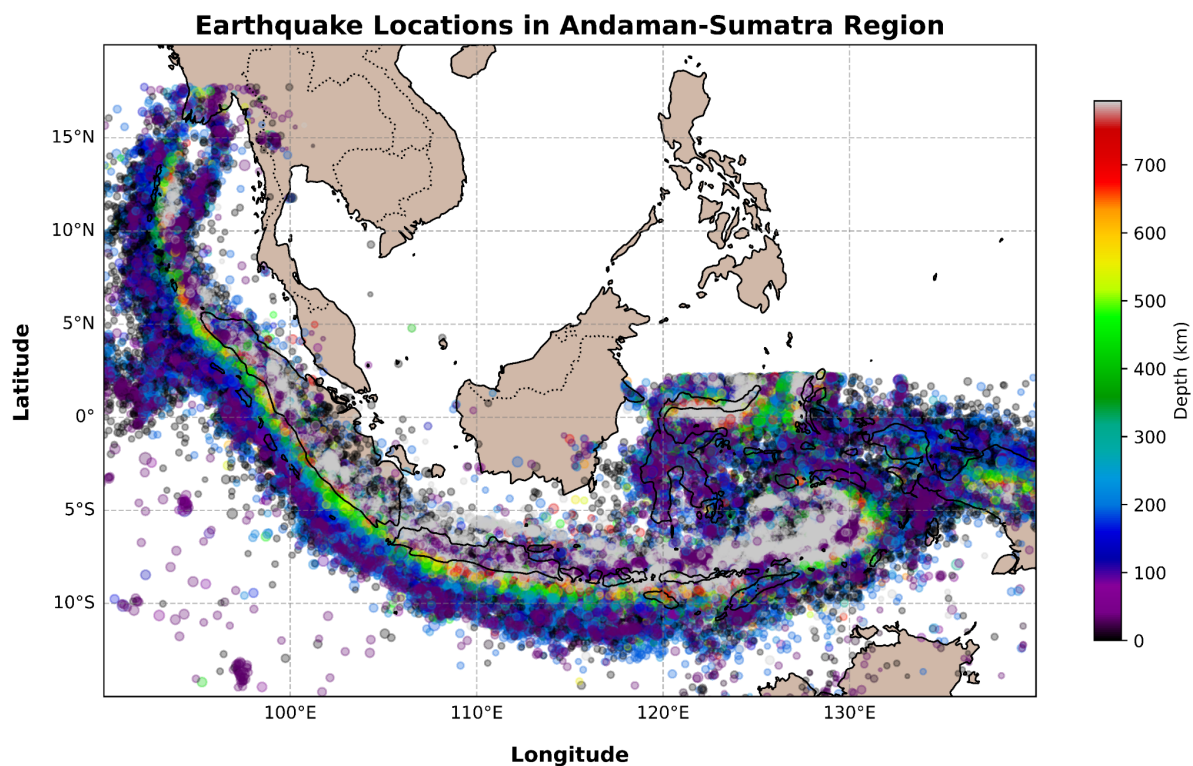


Fig.2: Visualization of seismic data in the Andaman-Sumatra Trench, showing the depth of recorded earthquakes.

The dataset for the region is given here. [Dataset](#)

A clear overview of the seismic activity in the region shows a dense spatial distribution of earthquake events. The earthquakes are plotted with their locations on a latitude-longitude grid, with depth represented by colour. The colour bar on the right indicates the depth of the earthquakes, ranging from 0 to over 700 kilometres. The pattern suggests significant tectonic activity along the depicted region, highlighting areas with higher seismic activity, particularly around the central curved belt, which indicates a subduction zone.

Earthquakes with Different Magnitudes Along Seafloor Age

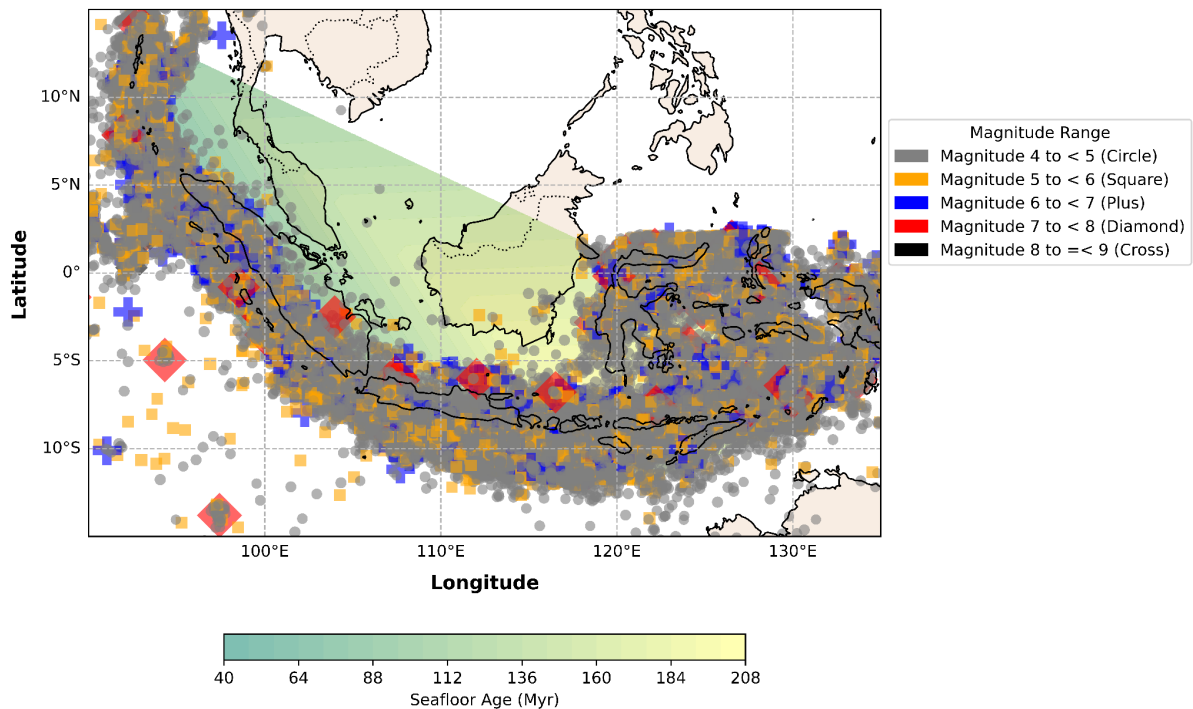


Fig.3: Epicenter map of Earthquakes above magnitude 4 and Subduction plate age for 1960-2024. This figure shows earthquake epicentres with subduction plate age in the Andaman Sea and Southeast Asia. The background color gradient represents seafloor age, from younger (green) to older (yellow). Earthquake markers and shapes vary in color based on magnitude.

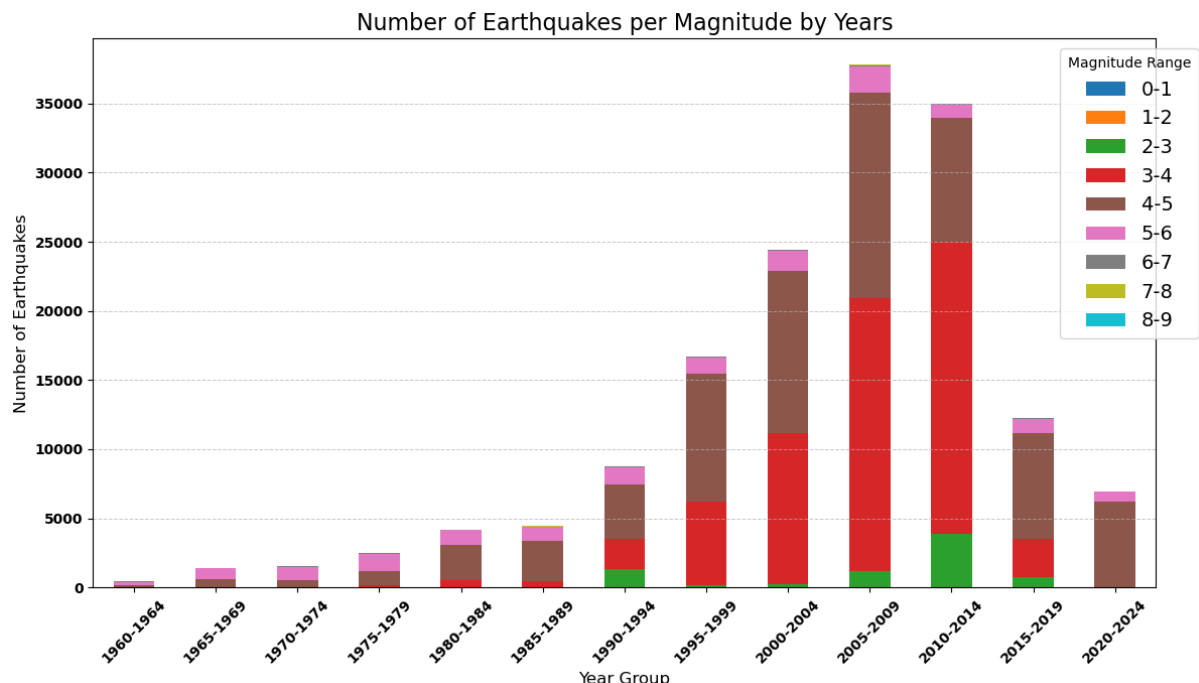


Fig.4: Shows the Frequency of earthquake magnitudes from 0 to 9 from 1960 to 2024.

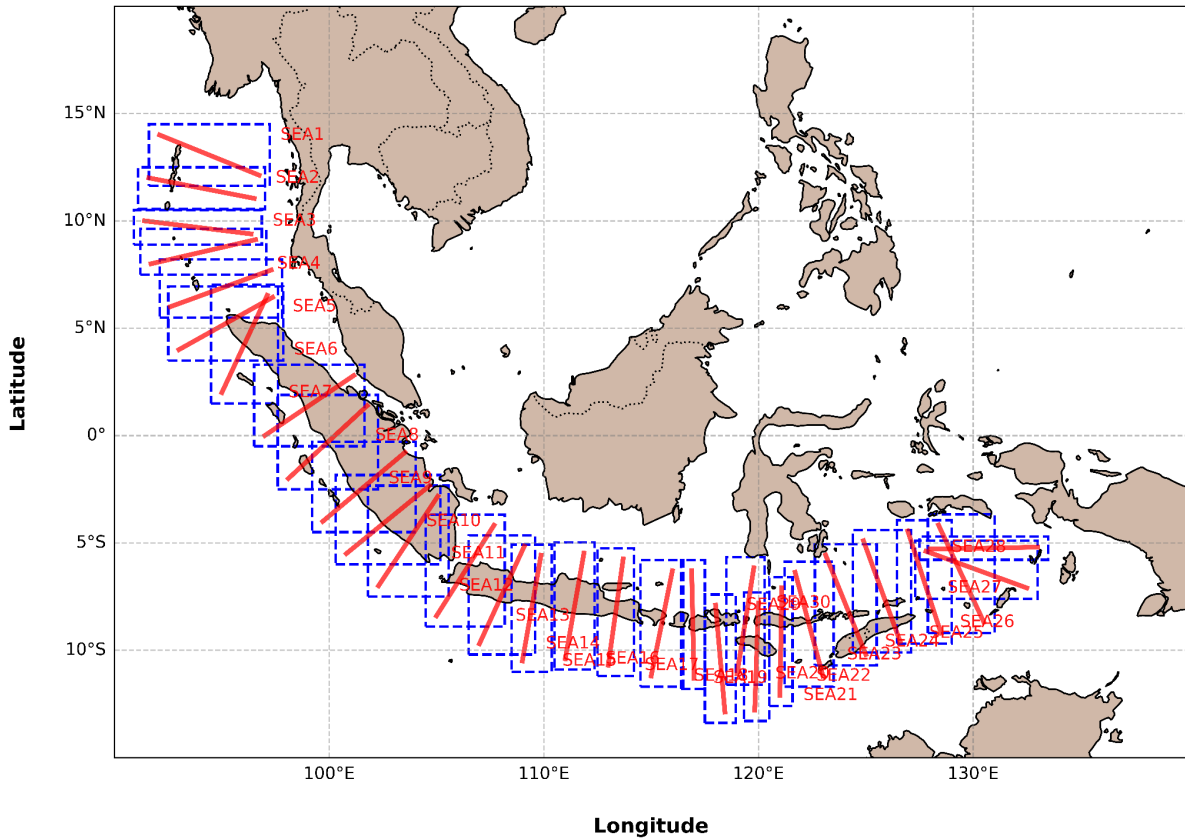


Fig.5: Shows the geographic distribution of study areas labelled SEA1, SEA2 and so on; the dashed blue rectangles indicate extensions of the dataset range.

Transects shown in Fig.5 provide detailed cross-sections of the trench, highlighting its geographical extent and boundaries. The displayed transects help to visualise the trench's structure and its relation to other tectonic features in the region.

Histograms were plotted for each segment of the Andaman Sea Transect, as shown in Fig. 6, focusing on extending the length of the transect (i.e. increasing the latitude and longitude for the region by 1 degree and making a rectangular box around the transect) to include a broader range of data points. The extended analysis of trench segments enabled us to compare the seismic behaviour across these sections, identifying areas with higher or lower seismic activity and understanding how underlying geological conditions might influence these variations.

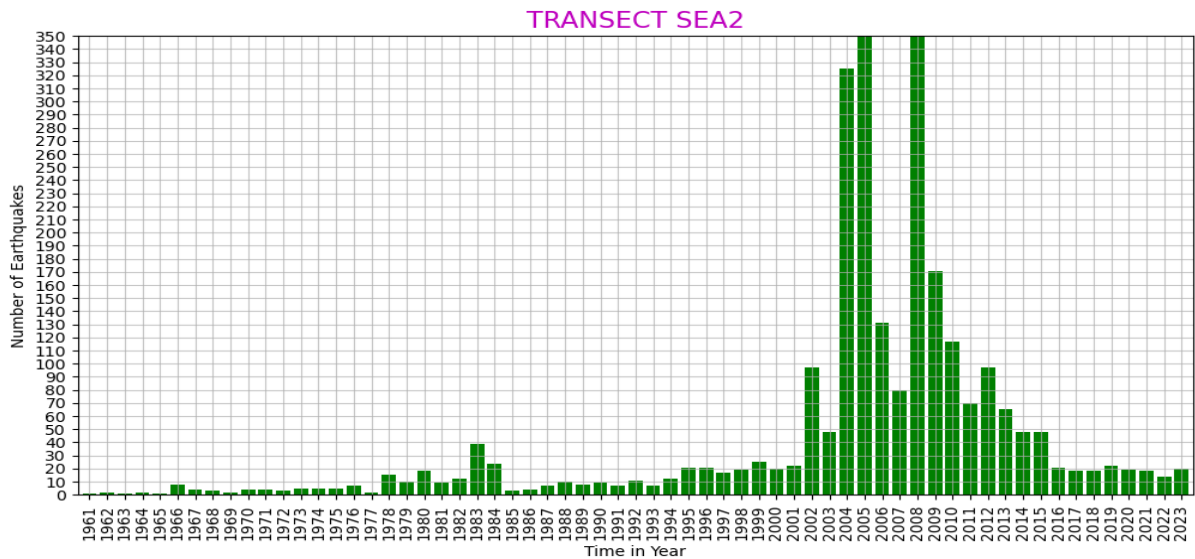
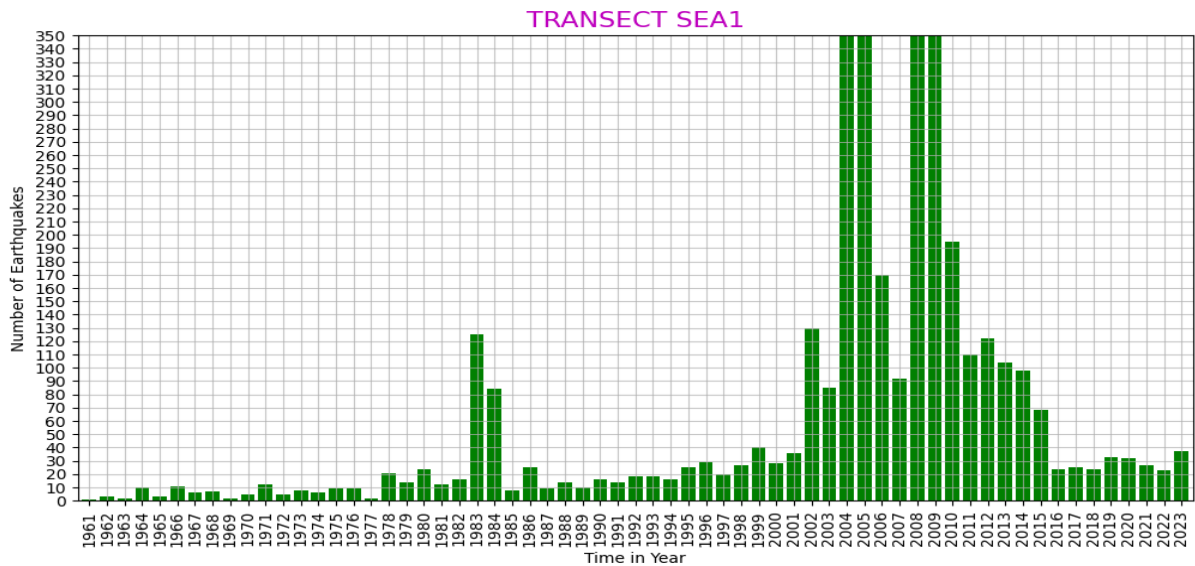


Fig.6: Histogram for transect SEA1 and SEA 2 Shows the number of earthquakes per year.

In this section, we show only two histogram plots. Additional histograms for all Transects can be found in [supplementary material](#). Each histogram was constructed to represent the number of earthquakes within the specific period of 1 year, providing a clear visual representation of the seismic activity of different transects, providing insights into patterns or variations along the subduction zone.

The transect depicted in Fig.5 presents various parameters essential for understanding the physical conditions influencing seismic activity in the Andaman region. These parameters can be categorised into three main groups: structural, slab, and kinematic.

Structural parameters include the [thickness of trench sediments](#) measured near the transect and [short-wavelength seafloor roughness](#), which provide insight into the subduction zone's geological features.

Slab parameters encompass the age of the subducting plate at the trench, which is vital for assessing the thermal and mechanical properties of the slab as it descends into the Earth's mantle.

Kinematic parameters cover several dynamic aspects of the subduction process, such as **subduction velocity**, which accounts for the deformation of the upper plate, and **convergence velocity** between the main tectonic plates. Additionally, the **deformation rate** of the plates is included to provide a more comprehensive understanding of the tectonic forces at play.

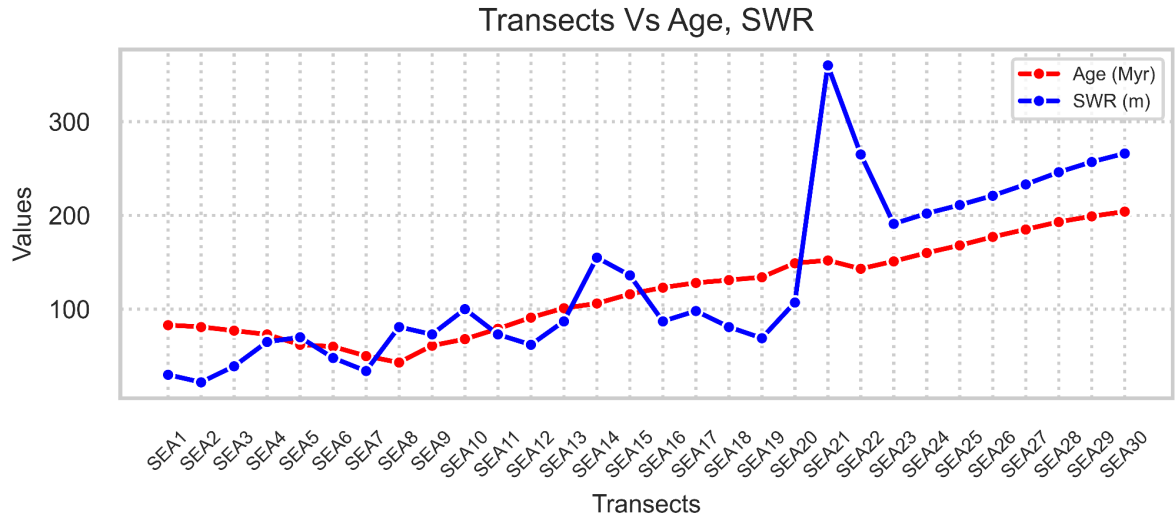


Fig.7: "Transects Vs Age, SWR" shows a comparison between **Subduction Plate Age** (Myr) and Short Wavelength Seafloor roughness (SWR, m) across transects SEA1 to SEA30. The red dashed line represents age, which gradually increases, while the blue dashed line represents SWR, showing significant fluctuation with a peak near SEA20.

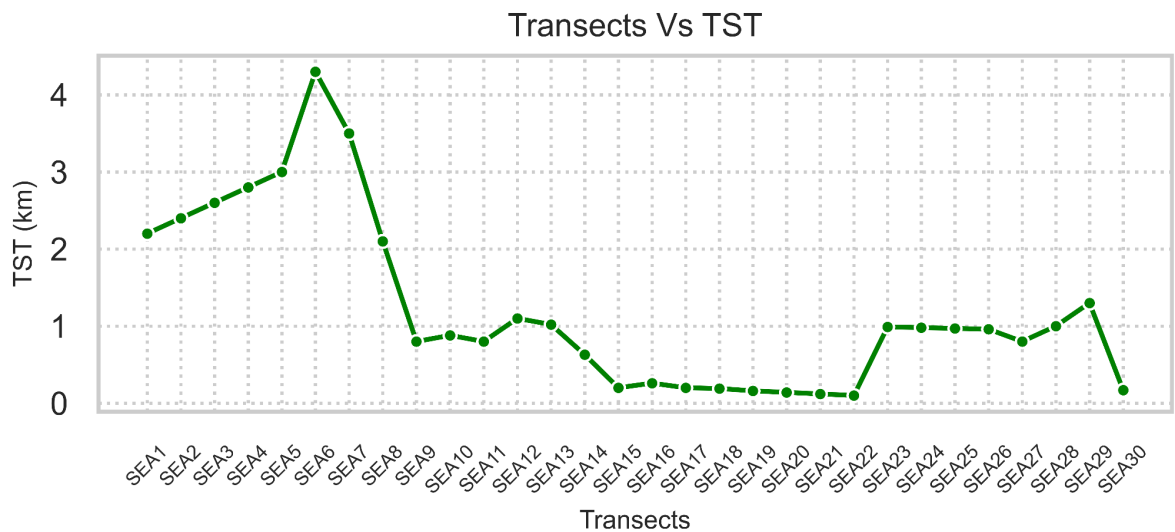


Fig.8: "Transects Vs TST" shows the variation of **Trench Sediment Thickness** (TST, km) across transects SEA1 to SEA30. The green line with circular markers highlights the TST

values, peaking around SEA8 and gradually decreasing with fluctuations across the remaining transects.

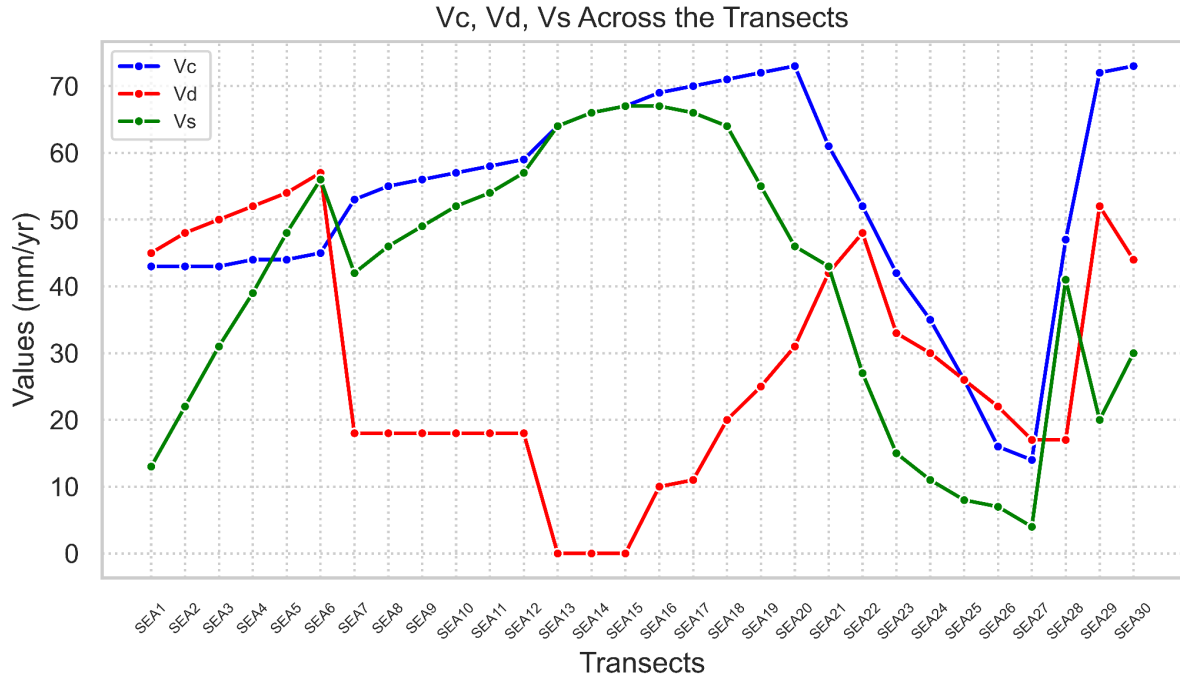


Fig.9: "Vc, Vd, Vs Across the Transects" compares the **Convergence, Divergence and Subduction velocity of plate** across transects SEA1 to SEA30. Each line fluctuates significantly across the transects, with the values ranging between 0 to 70 mm/yr. Peaks and troughs are visible, highlighting variations between the parameters along different transects.

These parameters were obtained using a tool designed for mapping subduction zones, available at [A Tool for Mapping Subduction Zones](#).

The sheet where all the parameters are listed is provided here: [Transect Parameters](#).

3. Methodology

3.1. ETAS Model:

The Epidemic Type Aftershock Sequence (ETAS) model is a mathematical framework used to describe the spatio-temporal clustering of earthquakes (Ogata, 1988). It posits that every earthquake, regardless of its size, can trigger subsequent earthquakes (aftershocks), which can trigger more, creating a cascading effect (Ogata, 1988, 1992). The model's foundation lies in the idea that all earthquakes, whether classified traditionally as foreshocks, mainshocks, or aftershocks, arise from the same underlying physical processes. The ETAS model quantifies the rate of earthquake occurrence at a specific time and location, conditioned on the history of past seismic activity. This conditional seismicity rate is expressed as:

$$\lambda(t, x, y|Ht) = \mu(x, y) + \sum g(t - t_i, x - x_i, y - y_i, m_i)t$$

where λ is the conditional seismicity rate, t is time, (x, y) is location, Ht is the history of earthquakes up to time t , $\mu(x, y)$ is the background seismicity rate (time-independent), g is the triggering function, modelling how past earthquakes influence future ones.

Background Seismicity Rate :

The Background Seismicity Rate represents the rate of earthquakes that occur independently of previous seismic events. These earthquakes are triggered by long-term tectonic loading rather than stress changes induced by prior earthquakes (Dieterich, 1994). Within the ETAS framework, the background seismicity rate is denoted by the symbol μ (mu) and is assumed to be spatially varying but time-independent. Estimating the background seismicity rate is crucial for understanding the overall seismic hazard and distinguishing between earthquakes caused by tectonic loading and those triggered by previous events. Background seismicity rates can exhibit spatial variations, reflecting the heterogeneous nature of the Earth's crust (Wiemer and Wyss, 2000). For example, several studies found that the background seismicity rate does not correlate with surface heat flow, suggesting that it is primarily driven by tectonic forces rather than fluid-related processes in the crust (Maeda, 1999). Background seismicity rate is often denoted in the number of earthquakes per square kilometre per day.

Productivity:

In the context of the ETAS model, productivity refers to the ability of an earthquake to trigger subsequent earthquakes (aftershocks). The productivity of an earthquake is influenced by several factors, including its magnitude and the stress conditions in the surrounding region(Felzer et al., 2002). The ETAS model quantifies productivity using the term as,

$$K(x, y)e^{a(x-y)(m_i - M_o)}$$

$K(x,y)$ is a coefficient that can vary spatially. $a(x,y)$ is the fertility exponent, representing how much more productive larger earthquakes are than smaller ones. m_i is the magnitude of the earthquake. M_o is the magnitude threshold above which earthquakes can trigger aftershocks.

The branching ratio, the average number of direct aftershocks triggered by an earthquake, is a key indicator of productivity(Helmstetter and Sornette, 2003). The spatial variability of the branching ratio suggests that the Earth's crust is not uniformly stressed, leading to variations in the triggering efficiency of earthquakes in different regions(Hainzl and Marsan, 2008). Productivity is a dimensionless quantity.

Temporal Decay :

In the context of the ETAS model, temporal decay describes how the rate at which an earthquake triggers aftershocks diminishes over time. The model captures this phenomenon

using the Omori kernel, a power-law function of the time elapsed since the mainshock (Nandan et al., 2021). The kernel's expression is:

$$\{t - t_i + c(x, y)\}^{(-1-\omega(x, y))}$$

where t is the current time, t_i is the time of the mainshock, $c(x, y)$ is a parameter that can vary spatially, and $\omega(x, y)$ is the temporal decay exponent, also potentially varying in space.

The Omori kernel dictates that the aftershock rate is highest immediately after the mainshock and decreases progressively over time. The rate of this decay is controlled by the exponent $\omega(x, y)$. The parameter $c(x, y)$ is often associated with the completeness of the earthquake catalog or the minimum time interval between a mainshock and its detectable aftershocks. The temporal decay exponent (ω) varies across regions and earthquake sequences, ranging from 0.6 to 2.5. This variability suggests that the physical processes governing aftershock decay might differ depending on the specific tectonic environment and characteristics of the mainshock. The ETAS model's ability to incorporate such variations in temporal decay allows it to capture the diverse aftershock patterns observed in real earthquake catalogs. It is also a dimensionless quantity.

Spatial Decay :

Spatial decay in the ETAS model refers to how the probability of an aftershock decreases as the distance from the mainshock increases(Ogata et al., 1995). The ETAS model captures this behaviour through a spatial kernel, a power-law function of the distance between the mainshock and a potential aftershock location.

The kernel's expression is:

$$\left\{ \left(x - x_i \right)^2 + \left(y - y_i \right)^2 + d \times (x, y) \times e^{((x,y) \times (m_i - M_0))} \right\}^{(-1-\rho(x, y))}$$

where (x, y) are the coordinates of the potential aftershock, (x_i, y_i) are the coordinates of the mainshock, $d(x, y)$, and $\rho(x, y)$ are parameters that can vary spatially, m_i is the magnitude of the mainshock, M_0 is the magnitude threshold above which earthquakes can trigger aftershocks, $\rho(x, y)$ is the spatial decay exponent, also potentially varying in space.

The spatial kernel describes the probability density of an aftershock occurring at a certain distance from the mainshock. The decay exponent $\rho(x, y)$ controls how rapidly this probability diminishes with distance. The term $d(x, y) \times e^{((x,y) \times (m_i - M_0))}$ allows the spatial extent of the aftershock zone to depend on the magnitude of the mainshock, with larger earthquakes potentially influencing a broader area. The spatial kernel, and thus the spatial decay component, is dimensionless. It is a scaling factor that modulates the aftershock rate

based on the distance from the mainshock. The unit of distance used in the spatial kernel is typically kilometres.

ETAS parameters include Temporal Decay (γ), Time Decay (c), Spacial distance (d), Background Seismicity (μ), Omori law Decay (τ), spacial Decay (ω), productivity (α) of aftershocks. These parameters were crucial for understanding the region's seismic clustering and aftershock patterns. ETAS parameters typically estimated from earthquake catalogs using statistical methods, allowing it to be used for forecasting future earthquake rates and assessing seismic hazard(Ogata, 1988).

3.2 ETAS inversion:

Inversion is performed using the **Expectation Maximization (EM) algorithm** proposed by Veen and Schoenberg (2008).

1. Initialization:

- The process starts with randomly chosen initial parameters (initial guess) for the ETAS model.

ETAS Parameters (theta_0): These are the assumed initial parameters for the ETAS model:

ETAS Parameters	assumed Initial parameters value for optimisation
log10_mu (μ): The background seismicity rate	-5.8
log10_k0: Productivity of aftershocks	-2.6
a: Magnitude scaling parameter	1.8
log10_c: Temporal aftershock decay constant	-2.5
omega (ω): A parameter related to spatial distribution decay	-0.02
log10_tau (τ): The temporal decay parameter	3.5
log10_d: Spatial decay constant	-0.85
gamma (γ): An exponent governing the spatial distribution of aftershocks	1.3
rho (ρ): Another spatial parameter influencing the shape of aftershock distribution	0.66

2. Expectation Step (E-step):

- For each earthquake event, probabilities are calculated to determine how likely it is that one event triggered another. This is done by considering the aftershock occurrence rates and the current parameter estimates.
- Additionally, each event is assigned an **independence probability**, the likelihood that the event occurred independently (not triggered by another event). These probabilities are based on the background seismicity rate.
- The **normalization factor** in the inversion algorithm ensures that all probabilities (triggering and independent) sum up to 1. Events in the auxiliary catalog (earlier period) can only be trigger events, while events in the primary catalog (the period of interest) can be both triggers and triggered events.

3. Maximization Step (M-step):

- The ETAS parameters are updated to maximize the **log-likelihood** of the observed earthquake data, given the expected number of independent events and aftershocks derived in the E-step.

4. Iteration:

- The algorithm alternates between the E-step and M-step until the parameters converge, meaning the changes between iterations become negligible.

This approach helps to find the best-fitting ETAS parameters for the earthquake catalog by repeatedly refining the estimates until a stable solution is reached.

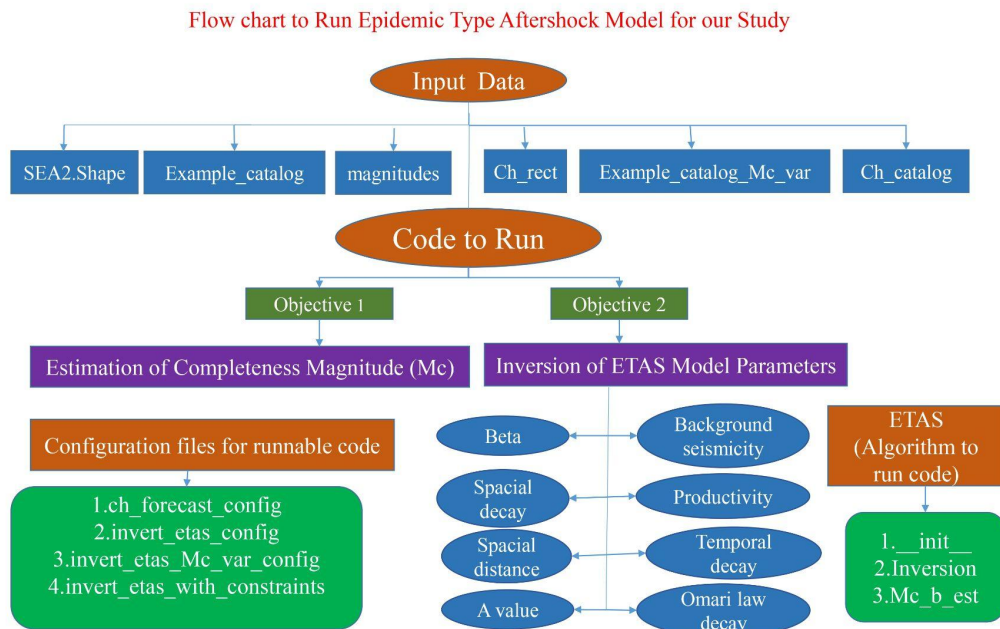


Fig.10: Flow chart of scripts required to run Epidemic-Type Aftershock Sequence model for our study.

The following directory structure and files appear as part of a system designed for running example inversions, particularly on earthquake data and model parameter estimation.

- **Input Data:** This directory contains the below files that serve as inputs for running the example inversions and simulations.
- **SEA2shape.npy:** This file contains the shape data for the **polygon** surrounding the region labelled SEA2. The shape represents the geographical boundary of a seismic zone.
- **ch_catalog.csv:** A catalog file listing seismic events from 1960 to 2024. This catalog includes event date-time, magnitudes, locations, and depths.
- **ch_rect.npy:** This file defines the shape of a **rectangular** region surrounding SEA2
- **example_catalog.csv:** A sample earthquake catalog containing events from 1960 to 2024 used as input for the invert_etas.py script. This file contains real earthquake event data, which will be used to calibrate the ETAS model parameters.
- **example_catalog_mc_var.csv:** Another sample catalog similar to example_catalog.csv, but intended to be used when varying the magnitude of completeness (Mc) during ETAS model inversion. This allows for the estimation of ETAS parameters under different assumptions about the completeness of the earthquake catalog.
- **magnitudes.npy:** A file containing an array of magnitudes used for Mc estimation.
- **Config:** This directory contains configuration files for running the scripts in the runnable_code/ directory.

□ **Code to run:**

- **estimate_mc.py:** This script estimates the constant completeness magnitude (mc) using the Expectation Maximization algorithm, the smallest magnitude above all earthquakes considered for Estimation of Mc, which is reliably detected.
- **invert_etas.py:** This script calibrates the parameters of the ETAS model based on an input earthquake catalog. The script includes options for varying the mc (completeness magnitude) and fixing certain parameters during the inversion process, allowing for flexible and robust parameter estimation.
- **ETAS:** This directory contains the core functions and algorithms for performing the ETAS model inversion and other related tasks, such as estimating the Mc value.
- **Output Data:** After running parameter inversions, Temporal Decay (γ), Time Decay (c), Spacial distance (d), Background Seismicity (μ), Omori law Decay (τ), spacial Decay (ω), productivity (α) parameters are obtained

The code for Epidemic type aftershock sequence model taken from <https://github.com/lmizrahi/etas>

Calculated ETAS parameters for all 30 Transects, as shown in Fig.5, can be found in [ETAS Parameters](#).

The ETAS parameters were then correlated with the transect parameters of the trench in the Andaman region to explore potential relationships between seismic activity and geological features. By analysing these correlations, it is identified how variations in trench characteristics may influence the frequency, distribution, and intensity of earthquakes in this region.

4. Result

Abbreviations for the below Plots:

Abbreviations	Unit
Age: Subducting Plate age	Million Years (Myr)
AWR: short wavelength roughness	Meter (m)
TST: Trench subduction thickness	Kilometer (Km)
Vc: Convergence velocity of plate	mm/yr
Vd: Divergence velocity of the plate	mm/yr
Vs: Subduction Velocity of the plate	mm/yr

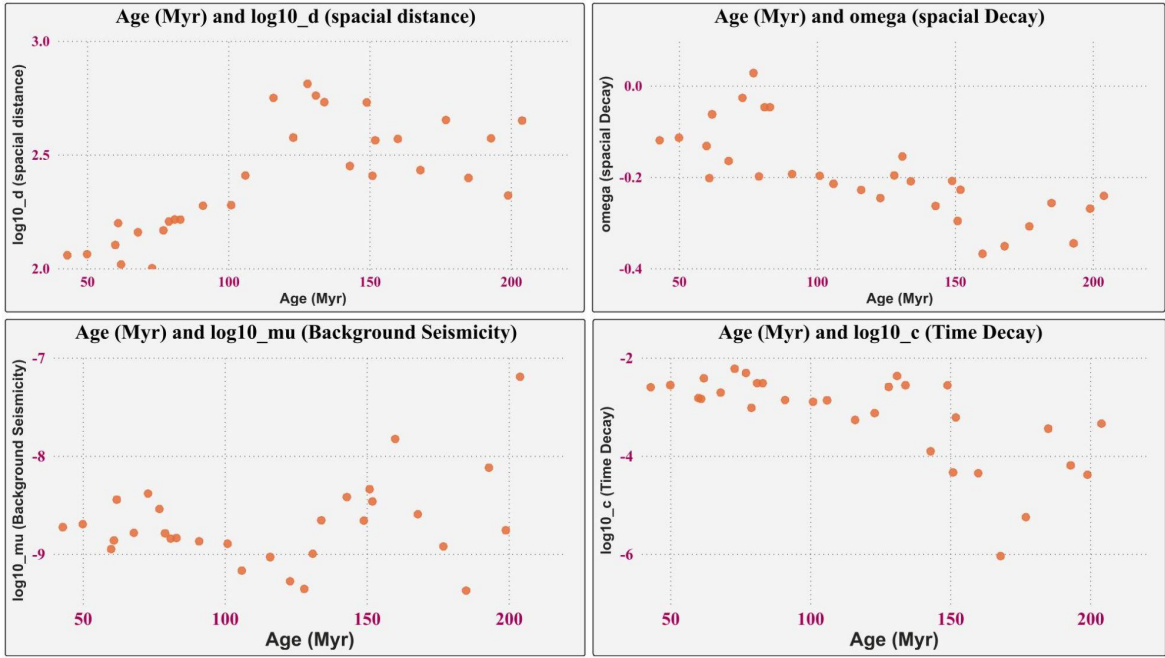


Fig.11: Shows four scatter plots examining the relationships of subducting plate Age (Myr) with spacial distance, spacial decay, background seismicity and time decay.

An increasing trend is seen between Age and $\log_{10}d$ (spatial distance), while no clear correlation is observed between Age and omega (spatial decay). A slight decrease is noted between Age and $\log_{10}\mu$ (background seismicity), and a significant decrease is evident between Age and $\log_{10}c$ (time decay).

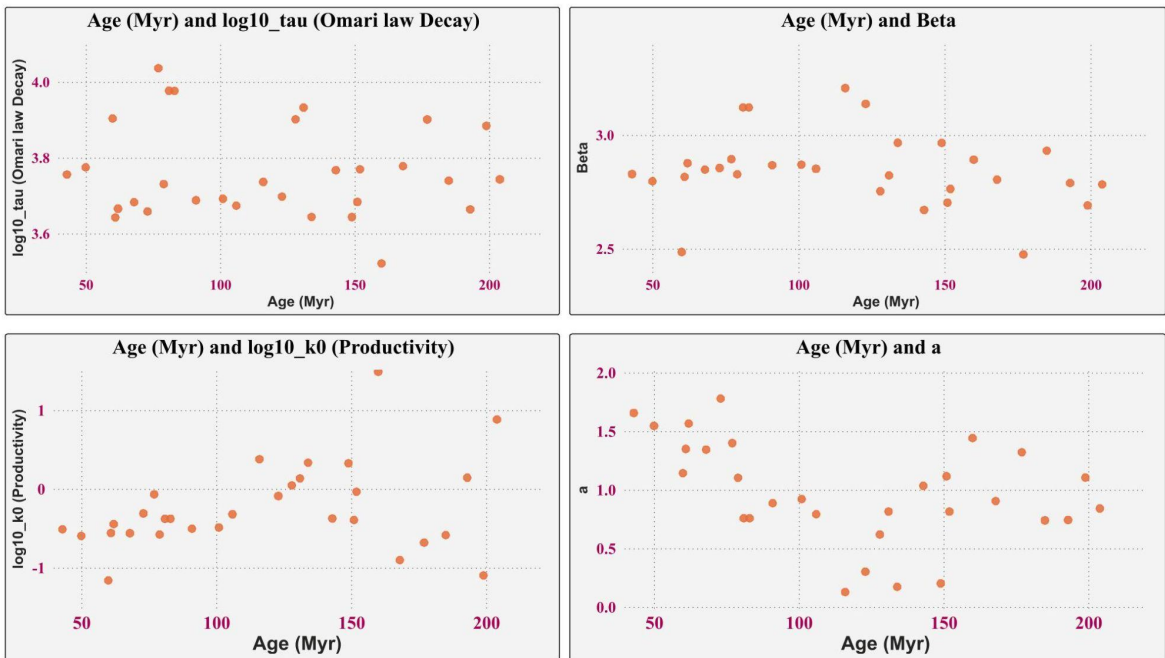


Fig.12: Shows four scatter plots analysing the relationships of Subductiong plate Age (Myr) with Omari law decay, beta, productivity and a value.

No clear trend is observed between Age and log10_tau (Omari law decay) or Age and "a," indicating no strong correlations. A slight decrease is noted in Beta with increasing age, while a weak, increasing trend is seen between Age and log10_k0 (Productivity).

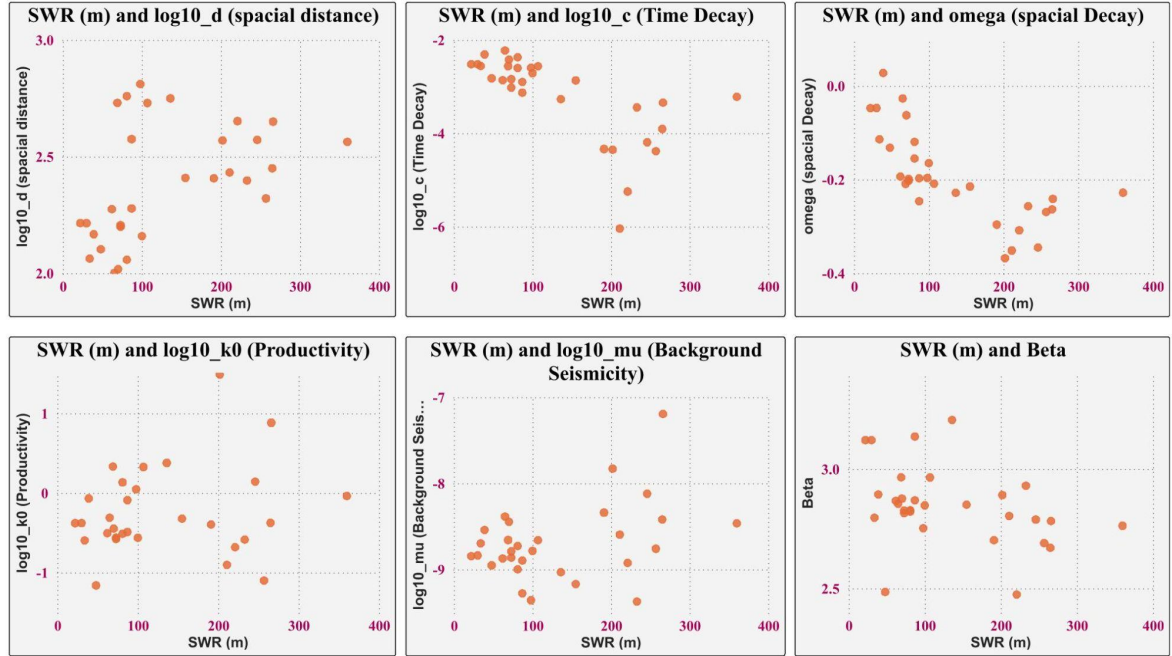


Fig.13: Shows six scatter plots examining the relationship of Short wavelength roughness (m) with spacial distance, time decay, spacial decay, productivity, background seismicity and beta.

There is no clear correlation between SWR and log10_d (spatial distance) or SWR and log10_k0 (Productivity). A negative correlation is observed between SWR and omega (spatial decay) and SWR and log10_mu (background seismicity). SWR also shows a weak decreasing trend with log10_c (Time Decay). However, there is no clear pattern between SWR and Beta.

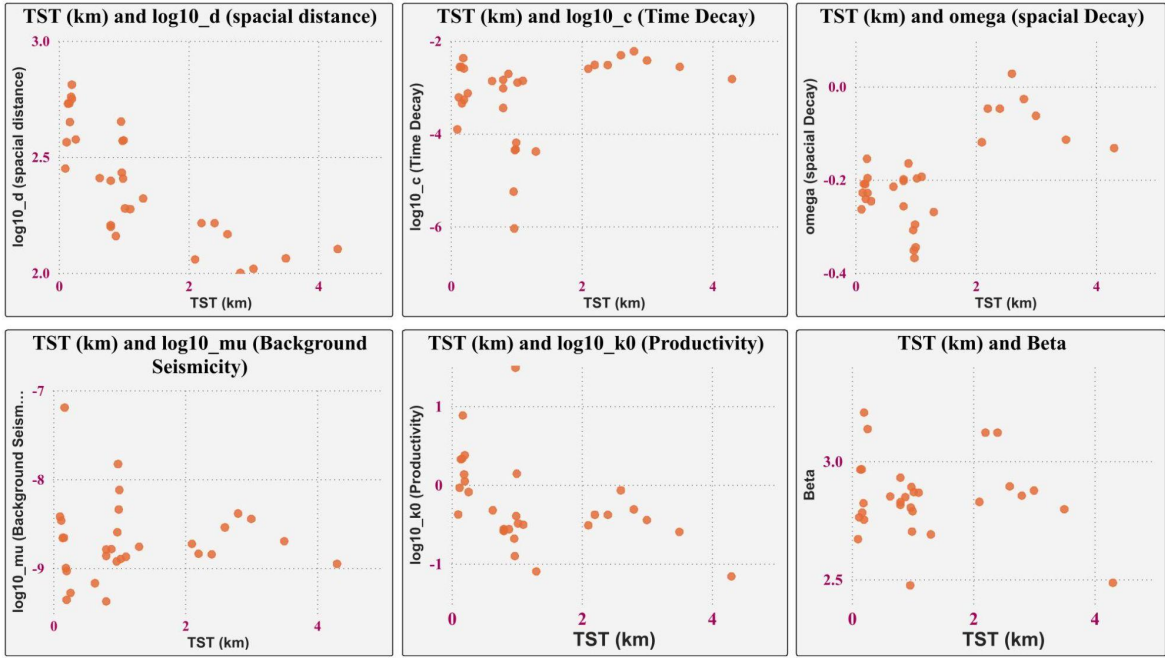


Fig.14: Six scatter plots examine the relationship of trench subduction thickness with spacial distance, time decay, spacial decay, productivity, background seismicity, and beta.

The correlation between TST (km) and other parameters is mostly negative. As TST increases, both $\log_{10}d$ (spatial distance), $\log_{10}\mu$ (background seismicity), and $\log_{10}k_0$ (productivity) decrease. The relationship between TST and $\log_{10}c$ (time decay) shows a weak negative trend, while omega (spatial decay) and Beta show no clear correlation with TST.

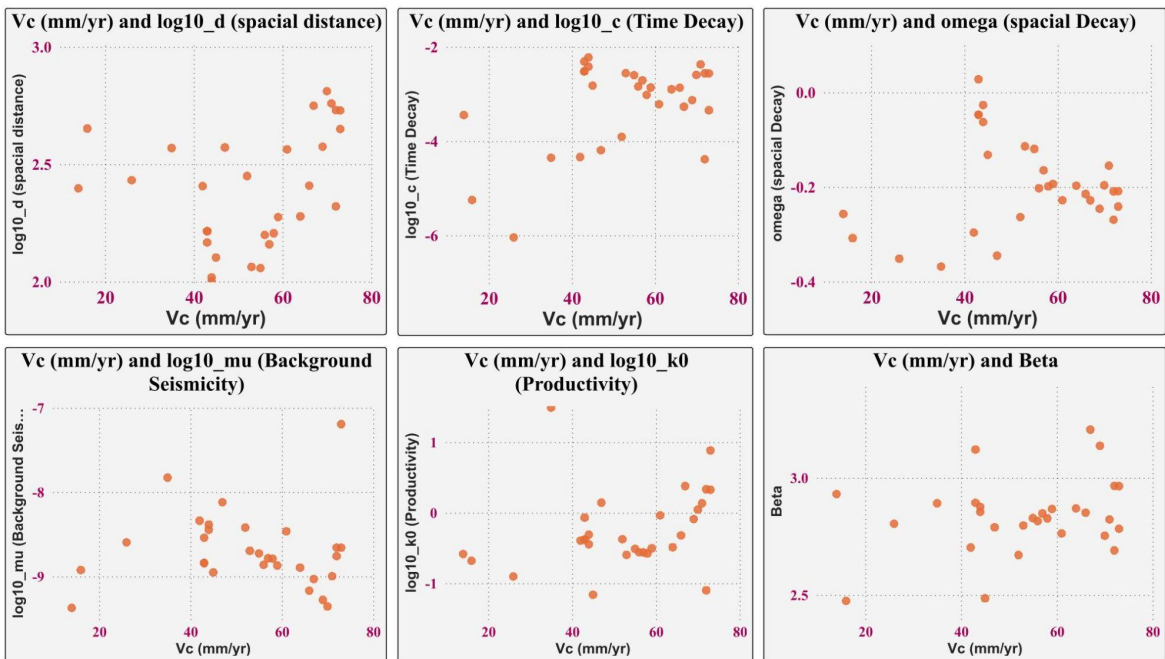


Fig.15: Six scatter plots are shown, examining the relationship of convergence velocity of the subducting plate with spatial distance, time decay, spacial decay, productivity, background seismicity, and beta.

V_c and $\log_{10} d$ (spatial distance) show a weak positive correlation, while V_c and $\log_{10} c$ (time decay) show a slight negative trend. The relationship between V_c and ω (spatial decay) seems unclear, with scattered points but a slight negative trend at higher values. There is a weak negative correlation between V_c and $\log_{10} \mu$ (background seismicity), while V_c and $\log_{10} k_0$ (productivity) show a weak positive correlation. V_c and Beta have no clear correlation.

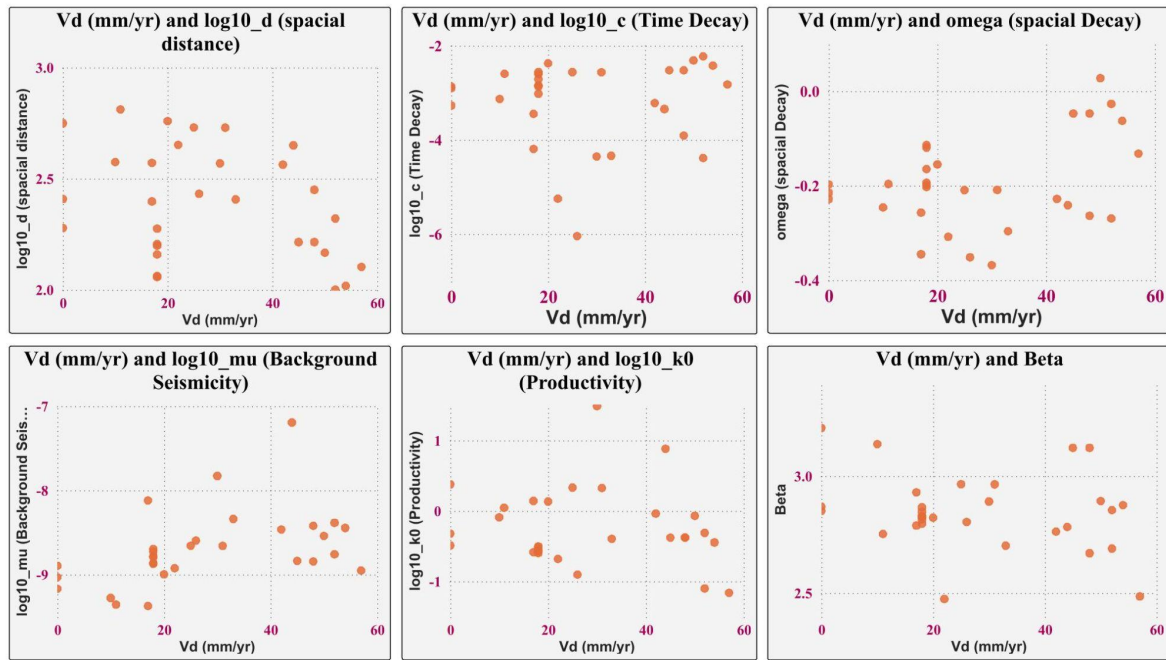


Fig.16: Six scatter plots are shown, examining the relationship of divergence velocity of the subducting plate with spatial distance, time decay, spacial decay, productivity, background seismicity, and beta.

V_d and $\log_{10} d$ (spatial distance) have a weak negative correlation, while V_d and $\log_{10} c$ (time decay) show no clear trend. The relationship between V_d and ω (spatial decay) is scattered but suggests a slight negative trend. V_d and $\log_{10} \mu$ (background seismicity) show no clear correlation, and V_d and $\log_{10} k_0$ (productivity) have a weak negative trend. V_d and Beta show no significant correlation.

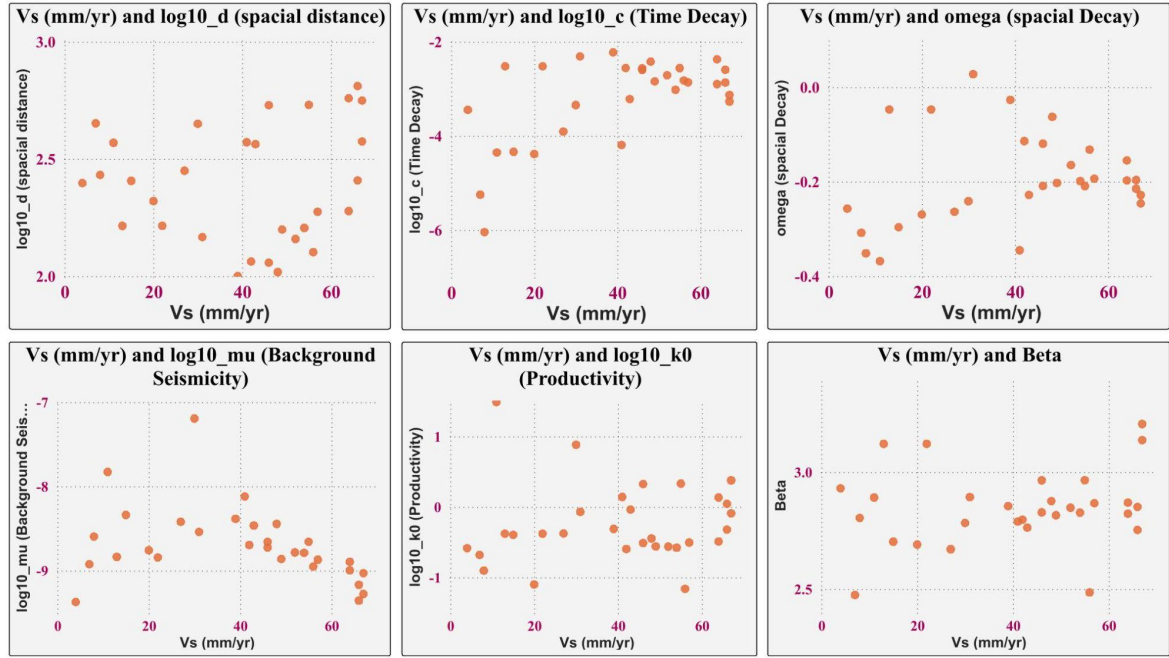


Fig.17: Six scatter plots are shown, examining the relationship of the subduction velocity of the plate with spatial distance, time decay, spatial decay, productivity, background seismicity, and beta.

Shows that as Vs increases, spatial distance tends to increase slightly. The plots of Vs against time decay and spatial decay show no clear correlation, with data points scattered widely. The background seismicity plot suggests a negative trend, where higher Vs values correspond to lower $\log_{10}\mu$ values. The relationship between Vs and productivity is unclear due to scattered data points, though there may be a slight positive trend. The plot of Vs versus beta also shows no distinct pattern or correlation.

The link for the PDF contains all these plots: [Correlations](#).

The ETAS model provided valuable parameters for understanding seismic activity in the Andaman Sea Trench. The key findings include:

1. **Spatial Distance (d):** A strong correlation was observed between the spatial distribution of aftershocks and the Oceanic plate age through visual inspection. As the **oceanic plate ages** (Steven Earle, “Physical Geology”), it becomes **denser and colder**, which may affect how stress is accumulated and released. This process makes the plate more rigid and **less prone to deformation**. Because of this, it might fracture differently, leading to a broader spread of seismic events.
2. **Temporal Decay (c):** A moderate correlation between temporal decay and oceanic plate age was found. **Older, more rigid plates tend to release accumulated stress over a more extended period**, resulting in a slower decay of aftershock activity. This slower time decay indicates that aftershocks persist longer but occur less frequently as time progresses after the mainshock.

5. Conclusion

This study successfully applied the ETAS model to earthquake data from the Andaman Sea Trench, sourced from the IRIS seismic database, and correlated the results with Transect Parameters. The observed correlations between seismicity and geological characteristics highlight the importance of integrating seismic models with geological data to improve regional hazard assessments.

6. All the links provided in the report:

Incorporated Research Institutions for Seismology (IRIS) -Website for the seismic Dataset	https://www.iris.edu/hq/
The dataset for the Andaman-Sumatra region is given here.	Dataset
Histogram plots for all the transects.	Histograms
A tool for mapping seduction zones.	https://submap.gm.umontpellier.fr/updates/
The sheet contains all geological parameters for the transects.	Transect Parameters
The sheet contains all the ETAS parameters for the transects.	ETAS Parameters
The reference code for the ETAS model.	https://github.com/lmizrahi/etas
The pdf contains all the correlational plots.	Correlation
My Github Repository.	https://github.com/StudentIITGN/M.Tech-Thesis

6. References

Curray JR (2005). Tectonics and history of the Andaman Sea region. J Asian Earth Sci 25:131–140

Spatial mapping of Gutenberg-Richters b-value [Version 1.3.0.1 \(615 KB\)](#) by [Yavor Kamer](#)

Mignon, A., J. Woessner (2012). Estimating the magnitude of completeness for earthquake catalogues, Community Online Resource for Statistical Seismicity Analysis, doi:10.5078/cross-00180805. Available at <http://www.corssa.org>.

Applying Conservation of Energy to Estimate Earthquake Frequencies from Strain Rates and Stresses Malte J. Ziebarth^{1,2}, Sebastian von Specht^{1,3}, Oliver Heidbach¹, Fabrice Cotton^{1,2}, and John G. Anderson⁴.

Utsu, T., & Ogata, Y. (1995). The centenary of the Omori formula for a decay law of aftershock activity. Journal of Physics of the Earth, 43(1), 1-33.

Nandan, S., Kamer, Y., Ouillon, G., Hiemer, S., and Sornette, D.: Global models for short-term earthquake forecasting and predictive skill assessment, Eur. Phys. J. Spec. Top., 230, 425–449, 2021.

Leila Mizrahi, Shyam Nandan, Stefan Wiemer 2021;
Embracing Data Incompleteness for Better Earthquake Forecasting. (Section 3.1)
Journal of Geophysical Research: Solid Earth; doi: <https://doi.org/10.1029/2021JB022379>

Leila Mizrahi, Shyam Nandan, Stefan Wiemer 2021;
The Effect of Declustering on the Size Distribution of Mainshocks.
Seismological Research Letters; doi: <https://doi.org/10.1785/0220200231>

*"Physical Geology" by Steven Earle used under a CC-BY 4.0 international license.

The proportionality between relative plate velocity and seismicity in subduction zones Satoshi Ide(DOI:10.1038/NGEO1901)

Variability of ETAS Parameters in Global Subduction Zones and Applications to Mainshock–Aftershock Hazard Assessment Lihong Zhang^{*1}, Maximilian J. Werner², and Katsuichiro Goda³.

SEISMIC PROPERTIES AND FRACTAL DIMENSION OF SUBDUCTION ZONE IN JAVA AND ITS VICINITY USING DATA FROM 1906 TO 2020 *Yunalia Muntafi^{1,2} and Nobuoto Nojima.

